

# Combined effects of local and nonlocal hybridization on formation and condensation of excitons in the extended Falicov-Kimball model

Pavol Farkašovský

Institute of Experimental Physics, Slovak Academy of Sciences  
Watsonova 47, 043 53 Košice, Slovakia

## Abstract

We study the combined effects of local and nonlocal hybridization on the formation and condensation of the excitonic bound states in the extended Falicov-Kimball model by the density-matrix-renormalization-group (DMRG) method. Analysing the resultant behaviours of the excitonic momentum distribution  $N(q)$  we found, that unlike the local hybridization  $V$ , which supports the formation of the  $q = 0$  momentum condensate, the nonlocal hybridization  $V_n$  supports the formation of the  $q = \pi$  momentum condensate. The combined effect of local and nonlocal hybridization further enhances the excitonic correlations in  $q = 0$  as well as  $q = \pi$  state, especially for  $V$  and  $V_n$  values from the charge-density-wave (CDW) region. Strong effects of local and nonlocal hybridization are observed also for other ground-state quantities of the model such as the  $f$ -electron density, or the density of unbound  $d$ -electrons, which are generally enhanced with increasing  $V$  and  $V_n$ . The same calculations performed for nonzero values of  $f$ -level energy  $E_f$  revealed that this model can yield a reasonable explanation for the pressure-induced resistivity anomaly observed experimentally in  $TmSe_{0.45}Te_{0.55}$  compound.

# 1 Introduction

The formation of excitonic quantum condensates is an intensively studied continuous problem in condensed matter physics [1–4]. Whilst theoretically predicted a long time ago [5], no conclusive experimental proof of the existence of the excitonic condensation has been achieved yet. However, the latest experimental studies of materials with strong electronic correlations showed that promising candidates for the experimental verification of the excitonic condensation could be  $TmSe_{0.45}Te_{0.55}$  [6],  $1T - TiSe_2$  [7],  $Ta_2NiSe_5$  [8], or a double bilayer graphene system [9]. In this regard, the mixed valence compound  $TmSe_{0.45}Te_{0.55}$  was argued to exhibit a pressure-induced excitonic instability, related to an anomalous increase in the electrical resistivity [6]. In particular, the detailed studies of the pressure-induced semiconductor-semimetal transition in this material (based on the Hall effect, electrical and thermal (transport) measurements) showed that excitons are created in a large number and condense below 20 K. On the other hand, in the layered transition-metal dichalcogenide  $1T - TiSe_2$ , a BCS-like electron-hole pairing was considered as the driving force for the periodic lattice distortion [7]. Moreover, quite recently, the excitonic-insulator state was probed by angle-resolved photoelectron spectroscopy in the semiconducting  $Ta_2NiSe_5$  compound [8]. At present, it is generally accepted that the minimal theoretical model for a description of excitonic correlations in these materials could be the Falicov-Kimball model [10] and its extensions [11–20]. The original Falicov-Kimball model describes a tight-binding system of itinerant  $d$  electrons interacting via the on-site Coulomb repulsion with localized  $f$  electrons (the spin degrees of freedom of the  $d$  and  $f$  electrons are not included):

$$H_0 = -t_d \sum_{\langle i,j \rangle} d_i^\dagger d_j + U \sum_i f_i^\dagger f_i d_i^\dagger d_i + E_f \sum_i f_i^\dagger f_i, \quad (1)$$

where  $f_i^\dagger$ ,  $f_i$  are the creation and annihilation operators for an electron in the localized state at lattice site  $i$  with binding energy  $E_f$  and  $d_i^\dagger$ ,  $d_i$  are the creation and annihila-

tion operators of the itinerant spinless electrons (with the nearest-neighbor  $d$ -electron hopping constant  $t_d$ ) in the  $d$ -band Wannier state at site  $i$ . In what follows we consider  $t_d = 1$  and all energies are measured in units of  $t_d$ .

Since the local  $f$ -electron number  $f_i^+ f_i$  is strictly conserved quantity, the  $d$ - $f$  electron coherence cannot be established in this model. One way to overcome this shortcoming is to include an explicit local hybridization  $H_V = V \sum_i d_i^+ f_i + f_i^+ d_i$  between the  $d$  and  $f$  orbitals. This model has been extensively studied in our previous work [20]. The numerical analysis of the excitonic momentum distribution  $N(q) = \langle b_q^+ b_q \rangle$  (with  $b_q^+ = (1/\sqrt{L}) \sum_k d_{k+q}^+ f_k$ , where  $L$  denotes the number of lattice sites) showed that this quantity diverges for  $q = 0$ , signaling a massive condensation of preformed excitons at this momentum. The stability of the zero-momentum ( $q = 0$ ) condensate against the  $f$ -electron hopping has been studied in our very recent paper [21]. It was found that the negative values of the  $f$ -electron hopping integrals  $t_f$  support the formation of zero-momentum condensate, while the positive values of  $t_f$  have the fully opposite effect. Moreover, it was shown that the fully opposite effects on the formation of condensate exhibit also the local and nonlocal hybridization with an inversion symmetry. The first one strongly supports the formation of condensate, while the second one destroys it completely. However, in the real  $d$ - $f$  systems, the on-site hybridization  $V$  is usually forbidden for parity reasons [22], and therefore the fact that the nonlocal hybridization with an inversion symmetry does not support the formation of excitonic condensate strongly limits the class of materials, where this phenomenon can be observed. In this situation, the most promising candidates for studying this phenomenon seem to be the systems with equal parity orbitals, where the nonlocal hybridization  $H_n$  can be written as:

$$H_n = V_n \sum_{\langle i,j \rangle} (d_i^+ f_j + H.c.). \quad (2)$$

In such systems, the local hybridization  $V$  is allowed, and thus one can examine the

combined effects of the local and nonlocal hybridization within the unified picture. The weak ( $U < 1$ ) and strong ( $V \ll U$  and  $V_n \ll U$ ) coupling limits of the model Hamiltonian  $H_0 + H_V + H_n$  have been analyzed recently by Zenker et al. in [23], and the corresponding mean-field quantum phase diagrams were presented as functions of the model parameters  $U, V, V_n$  and  $E_f$  for the half-filled band case  $n_f + n_d = 1$  and  $D = 2$ . Moreover, examining effects of the local  $V$  and nonlocal  $V_n$  hybridization they found that in the pseudospin space ( $c_{i\uparrow}^+ = d_i^+, c_{i\downarrow}^+ = f_i^+$ ) the nonlocal hybridization  $V_n$  favors the staggered Ising-type ordering along the  $x$  direction, while  $V$  favors a uniform polarization along the  $x$  direction and the staggered Ising-type ordering along the  $y$  direction.

In the current paper we examine model for arbitrary  $V$  and  $V_n$  and unlike the paper of Zenker et al. [23] we focus our attention primarily on a description of process of formation and condensation of excitonic bound states. For this reason we calculate (by the DMRG method) various ground state characteristics of the model such as the excitonic momentum distribution  $N(q)$ , the density of zero momentum excitons  $n_0 = \frac{1}{L}N(q = 0)$ , the total exciton density  $n_T = \frac{1}{L}\sum_q N(q)$ , the total  $d$ -electron density  $n_d$  and the total density of unbound  $d$  electrons  $n_d^{un} = n_d - n_T$ , and analyze their behaviours as functions of the local/nolocal hybridization and the  $f$ -level position  $E_f$ . It should be noted that such a study could be very valuable from the point of view of real materials, since taking into account the parametrization between the external pressure and the position of the  $f$  level ( $E_f \sim p$ ), one could deduce from the  $E_f$  dependencies of the ground state characteristics also their  $p$  dependencies, at least qualitatively [25]. As shown at the end of this paper a simple model based on the above mentioned parametrization can yield a reasonable explanation for the pressure-induced resistivity anomaly observed experimentally in  $TmSe_{0.45}Te_{0.55}$  compound [6].

## 2 Results and discussion

### 2.1 DMRG results

To examine combined effects of the local  $V$  and nonlocal  $V_n$  hybridization on the formation and condensation of excitonic bound states in the extended Falicov-Kimball model we have performed exhaustive DMRG studies of the model Hamiltonian  $H = H_0 + H_V + H_n$  for a wide range of the model parameters  $V, V_n$  and  $E_f$  at the total electron density  $n = n_d + n_f = 1$  (the half-filled band case). In all examined cases we typically keep up to 500 states per block, although in the numerically more difficult cases, where the DMRG results converge slower, we keep up to 1000 states. Truncation errors [26], given by the sum of the density matrix eigenvalues of the discarded states, vary from  $10^{-6}$  in the worse cases to zero in the best cases.

Let us start a discussion of our numerical results for the case  $E_f = 0$ . The typical examples of the excitonic momentum distribution  $N(q)$  calculated for the representative values of  $V, V_n$  and  $U$  are summarized in Fig. 1, where different panels correspond to: (a)  $V = 0$  and  $V_n \geq 0$ , (b)  $V_n = 0$  and  $V \geq 0$ , (c)  $V > 0$  and  $V_n \geq 0$ . Comparing these behaviours one can see that the local and nonlocal hybridization exhibit fundamentally different effects on the formation and condensation of excitonic bound states. While the local hybridization supports the formation of the zero-momentum (ferroelectric) condensate, the nonlocal hybridization supports the formation of the  $\pi$ -momentum (antiferroelectric) condensate. This is supported by the finite size scaling analysis of the excitonic momentum distribution  $N(q)$  and the densities of  $q = 0$  and  $q = \pi$  momentum excitons in Fig. 1d. With the increasing cluster size the excitonic momentum distribution  $N(q)$  diverges at  $q = 0$  as well as  $q = \pi$  and both, the density of the zero-momentum condensate ( $n_0 = N(0)/L$ ) as well as the density of the  $\pi$ -momentum condensate ( $n_\pi = N(\pi)/L$ ) have the finite values at singular points of  $N(q)$  (see the insets in Fig. 1d).

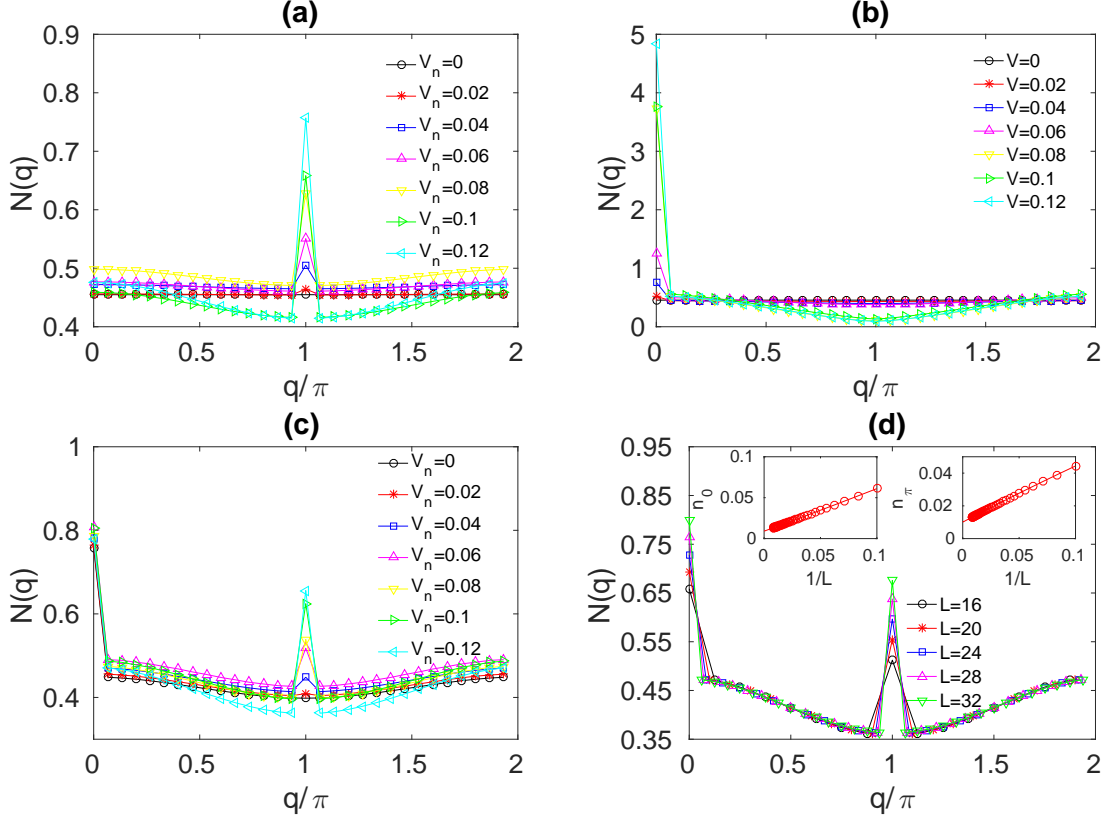


Figure 1: The DMRG results for the excitonic momentum distribution  $N(q)$  calculated for different model parameters. (a)  $N(q)$  calculated for  $V = 0, U = 4, E_f = 0, L = 30$  and different values of  $V_n$ . (b)  $N(q)$  calculated for  $V_n = 0, U = 4, E_f = 0, L = 30$  and different values of  $V$ . (c)  $N(q)$  calculated for  $V = 0.04, U = 4, E_f = 0, L = 30$  and different values of  $V_n$ . (d)  $N(q)$  calculated for  $V = 0.04, V_n = 0.12, U = 4, E_f = 0$  and different values of  $L$ . The insets show the densities of  $q = 0$  and  $q = \pi$  momentum excitons as functions of  $1/L$  calculated for the same values of model parameters.

Let us now discuss the combined effect of local and nonlocal hybridizations on the other ground state quantities of the model. To describe, in more detail, the process of formation of excitonic bound states for nonzero  $V$  and  $V_n$ , we have plotted in Fig. 2, the density of zero momentum excitons  $n_0$ , the density of  $q = \pi$  momentum excitons  $n_\pi$ , the total  $d$ -electron density  $n_d$  and the total density of unbound  $d$  electrons  $n_d^{un} = n_d - n_T$  as functions of nonlocal hybridization  $V_n$  for  $U = 4, E_f = 0$  and several different values of  $V$ . Fig. 2a shows the dependence of the density of zero-momentum excitons  $n_0$  on  $V_n$ . One can see that the density of the zero-momentum excitons  $n_0$  as a function of nonlocal hybridizations  $V_n$  exhibits two different types of behaviours. While for

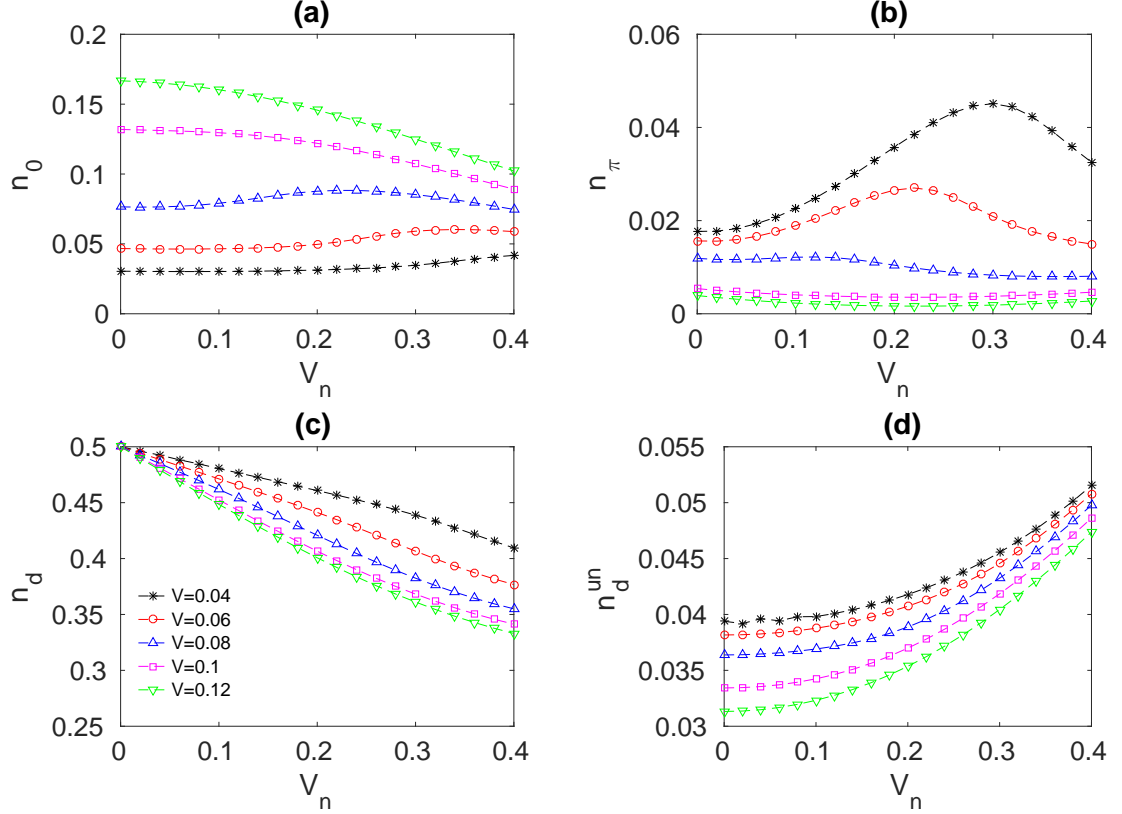


Figure 2: The density of zero-momentum excitons  $n_0$  (a), the density of  $\pi$ -momentum excitons  $n_\pi$  (b), the total  $d$ -electron density  $n_d$  (c), and the total density of unbound  $d$  electrons  $n_d^{\text{un}} = n_d - n_T$  (d) as functions of  $V_n$  calculated for  $U = 4, E_f = 0, L = 60$  and five different values of  $V$ .

sufficiently large values of  $V$  ( $V > 0.1$ ), the number of zero-momentum excitons is suppressed with the increasing values of nonlocal hybridization  $V_n$ , in the opposite limit  $V < 0.1$ , the number of zero-momentum excitons increases for nonlocal hybridizations smaller than some critical nonlocal hybridization  $V_n^c$  and decreases above this value. To reveal the nature of different behaviour of  $n_0(V_n)$  below and above  $V$  we have calculated numerically the Fourier transform of the  $f$ -electron density-density correlation function  $S(q)$  defined by

$$S(q) = \frac{1}{L} \sum_{jl} e^{iqL} (\langle n_j^f n_{j+l}^f \rangle - \langle n_j^f \rangle \langle n_{j+l}^f \rangle). \quad (3)$$

In the regime of long-range order  $S(q = \pi) \equiv S(\pi)$  scales linearly with  $L$  and above this regime  $S(\pi)$  undergoes a rapid change (see Fig.3a), that indicates the transition from the ordered to homogeneous phase. Following the procedure described in detail

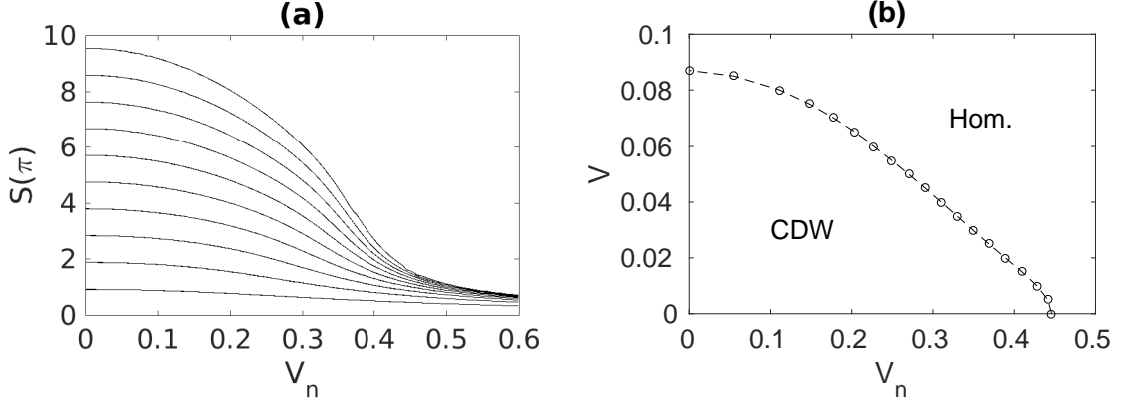


Figure 3: a) The Fourier transform of the  $f$ -electron density-density correlation function  $S(\pi)$  as a function of nonlocal hybridization  $V_n$ , calculated for  $U = 4, E_f = 0, V = 0.04$  and several different values of  $L$  (from bottom to top  $L=4, 8, 12 \dots 40$ ). b) The ground-state phase diagram of the model in the  $V_n$ - $V$  plane calculated for  $U = 4, E_f = 0, L = \infty$ . Two different regions correspond to the charge density wave (CDW) and homogeneous (Hom.) phase.

in our previous work [20], we have used  $S(\pi)$  to identify the phase boundary between the long-range order (CDW) state and the homogeneous phase in the  $V_n$ - $V$  plane. The complete phase diagram of the model obtained for  $U = 4$  is displayed in Fig. 3b and it clearly demonstrates that different behaviour of  $n_0(V_n)$  below and above  $V$  is obviously caused by the CDW order, which supports formation of the zero-momentum condensate. The CDW order is apparently responsible also for an anomalous increase in the density of  $q = \pi$  momentum excitons observed for  $V$  and  $V_n$  small (see Fig. 2b)

The strong combined effects of the local and nonlocal hybridization are observed also for the  $d$ -electron density as a function of  $V_n$  (see Fig. 2c). While for  $V = 0$  the  $d$ -electron density does not depend on the nonlocal hybridization  $V_n$  ( $n_d = 0.5$  for all  $V_n$ ), for finite values of local hybridization the  $d$ -electron density is considerably reduced by the increasing nonlocal hybridization. Since the  $f$ -electron density  $n_f$  is simply given by  $n_f = 1 - n_d$  one obtains the nonlocal hybridization induced valence transitions even for the case  $E_f = 0$ , that in the absence of nonlocal hybridization corresponds to the half-filled band case  $n_f = n_d = 1/2$ . A very important quantity that characterizes the ground state of the model is the density of unbound electrons

$n_d^{un} = n_d - n_T$ . Its behaviour is shown in Fig. 2d and one can see that this quantity is considerably enhanced by the nonlocal hybridization.

However, from the physical point of view, it is the most interesting to examine changes of  $n_0, n_\pi, n_d$  and  $n_d^{un}$  as functions of the  $f$ -level position  $E_f$ , since taking into account the parametrization between the external pressure  $p$  and the  $f$ -level energy  $E_f$  [25], such a study can give us the answer to the very important question, and namely, how these quantities change with applied pressure  $p$ . In Fig. 4 we present the resultant behaviours of  $n_0, n_\pi, n_d, n_d^{un}$  as functions of the  $f$ -level position  $E_f$  obtained by the DMRG method for  $V = 0.2$  and several different values of  $V_n$ . In all examined

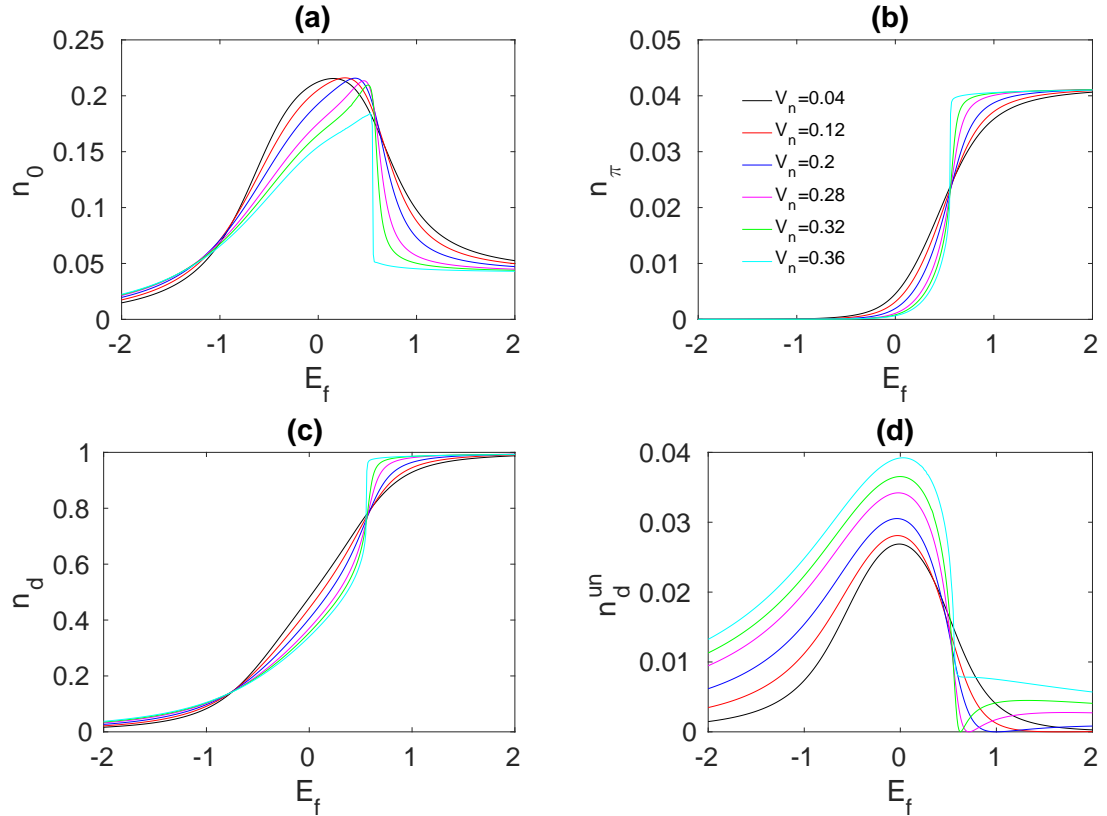


Figure 4: The density of zero-momentum excitons  $n_0$  (a), the density of  $\pi$ -momentum excitons  $n_\pi$  (b), the total  $d$ -electron density  $n_d$  (c), and the total density of unbound  $d$  electrons  $n_d^{un} = n_d - n_T$  (d) as functions of  $E_f$  calculated for  $U = 4, V = 0.2, L = 60$  and six different values of  $V_n$ .

cases, the density of zero-momentum excitons is the most significantly enhanced for  $d$ -electron densities near the half-filled band case  $E_f = 0$  and  $n_d = 1/2$ . The changes

of  $n_0$  are gradual for  $E_f < 0$  and very steep, but still continuous, for  $E_f > 0$ . The fully different behaviour exhibits the density of  $\pi$ -momentum excitons  $n_\pi$ . Its enhancement with increasing  $E_f$  is practically negligible for  $E_f < 0$ , but from this value  $n_\pi$  starts to increase sharply and tends to its saturation value corresponding to the fully occupied  $d$  band  $n_d \sim 1$ . The density of unbound  $d$  electrons  $n_d^{un}$  exhibits very simple behaviour for  $E_f < 0$ . In this limit  $n_d^{un}$  gradually increases with increasing  $E_f$  for all examined values of nonlocal hybridization  $V_n$ . However, in the opposite case ( $E_f > 0$ ) the density of unbound  $d$  electrons  $n_d^{un}$  behaves fully differently for  $V_n < V_n^c$  and  $V_n > V_n^c$ , where  $V_n^c \sim 0.2$ . For  $V_n < V_n^c$  the density of unbound  $d$  electrons  $n_d^{un}$  gradually decreases with increasing  $E_f$  and tends to zero when  $E_f$  approaches the upper edge of the noninteracting band  $E_f = 2$ , but in the opposite limit the density of unbound  $d$  electrons  $n_d^{un}$  decreases on the interval of  $E_f$  values from  $E_f = 0$  to  $E_f^c(V_n)$ , and  $n_d^{un}$  starts to increase again for  $E_f > E_f^c(V_n)$ . Taking into account the above mentioned parametrization between  $E_f$  and the external pressure  $p$ , as well as the fact that the electrical conductivity is proportional to the density of unbound electrons  $n_d^{un}$  (and the electrical resistivity to  $1/n_d^{un}$ ), the results discussed above could have very important physical consequences. Indeed, in Fig. 5 we have plotted the quantity  $1/n_d^{un}$  (in the logarithmic scale) as a function of  $E_f$  and compare it with experimental measurements of the pressure dependence of the electrical resistivity in mixed valence compound  $TmSe_{0.45}Te_{0.55}$  (see the inset in Fig. 5). One can see that there is a nice qualitative accordance between our theoretical predictions and experimental results of Wachter et al. [6]. In spite of the fact that our model is in many aspects very simplified, the physics that could lead to the unusual behaviour of the electrical resistivity in  $TmSe_{0.45}Te_{0.55}$  under the external pressure seems to be clear. This is a result a formation and condensation of excitonic bound states of conduction-band electrons and valence-band holes.

In summary, the combined effects of local and nonlocal hybridization on the forma-

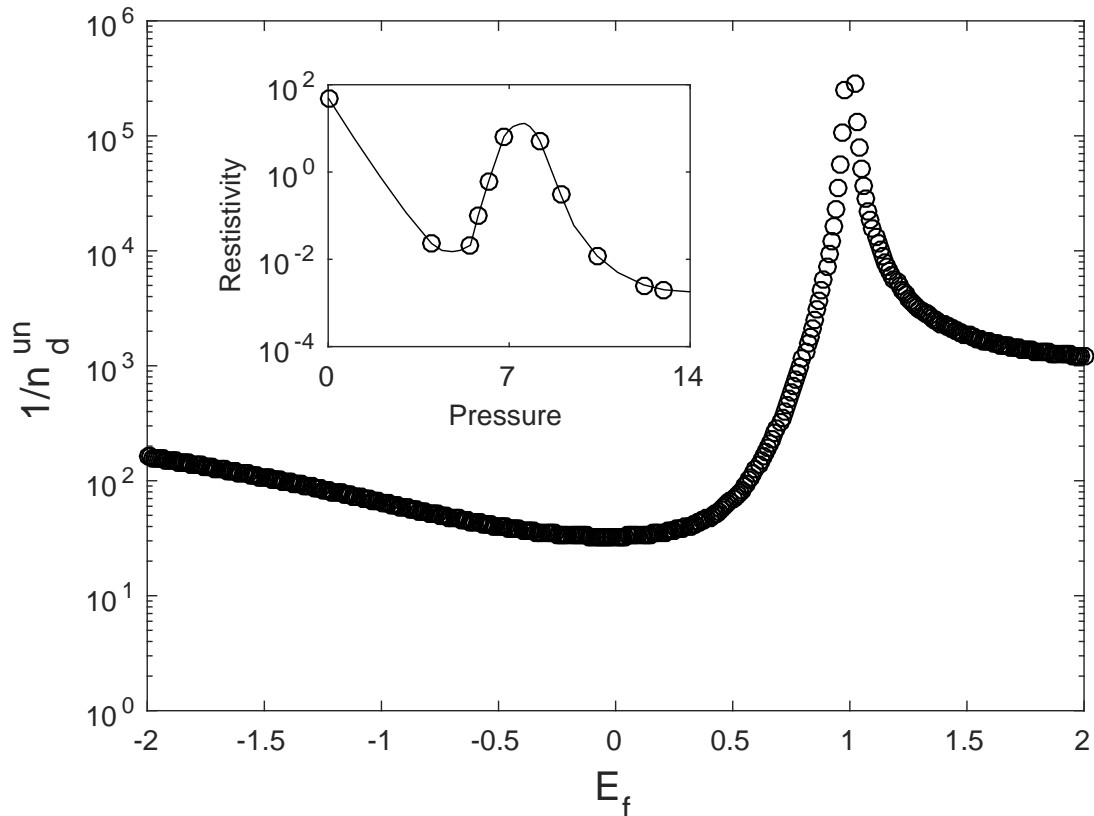


Figure 5: The inverse value of the density of unbound  $d$ -electrons  $n_d^{un}$  as a function of the  $f$ -level energy  $E_f$  calculated for  $U = 4, V = 0.2, V_n = 0.2$  and  $L = \infty$ . The inset shows the resistivity as the function of pressure in  $TmSe_{0.45}Te_{0.55}$  at 4.2 K [6].

tion and condensation of the excitonic bound states in the extended Falicov-Kimball model have been studied by DMRG method. The analysis of the resultant behaviours of the excitonic momentum distribution  $N(q)$  showed that (i) the local hybridization  $V$  supports the formation of the ferroelectric  $q = 0$  momentum condensate and the nonlocal hybridization  $V_n$  supports the formation of the antiferroelectric  $q = \pi$  momentum condensate, (ii) the combined effect of local and nonlocal hybridization further enhances the excitonic correlations in  $q = 0$  as well as  $q = \pi$  state, especially for  $V$  and  $V_n$  values from the CDW region, (ii) strong effects of local and nonlocal hybridization are observed also for other ground-state quantities of the model such as the  $f$ -electron density, or the density of unbound  $d$ -electrons, which are generally enhanced with in-

creasing  $V$  and  $V_n$  ( $E_f = 0$ ), (iv) the model can yield a reasonable explanation for the pressure-induced resistivity anomaly observed experimentally in  $TmSe_{0.45}Te_{0.55}$  compound.

This work was supported by Slovak Research and Development Agency (APVV) under Grant APVV-0097-12 and ERDF EU Grants under the contract No. ITMS 26220120005 and ITMS26210120002.

## References

- [1] J.M. Blatt, K.W. Böer, and W. Brandt, Phys. Rev. **126**, 1691 (1962)
- [2] L.V. Keldysh and H.Y.V. Kopaev, Sov. Phys. Sol. State **6**, 2219 (1965).
- [3] S.A. Moskalenko and D.W. Snoke, *Bose-Einstein Condensation of Excitons and Biexcitons* (Cambridge Univ. Press, Cambridge,2000).
- [4] P.B. Littlewood, P.R. Eastham, J.M.J. Keeling, F.M. Marchetti D.B. Simons, and M.H. Szymanska, J. Phys. Condens. Matter **16**, S3597 (2004).
- [5] J. des Cloizeaux, J. Phys. Chem. Solids **26**, 259 (1965).
- [6] J. Neuenschwander and P. Wachter, Phys. Rev. **41**, 12693 (1990); B. Bucher, P. Steiner and P. Wachter, Phys. Rev. Lett. **67**, 2717 (1991).
- [7] C. Monney, G. Monney, P. Aebi, and H. Beck, Phys. Rev. **B85**, 235150 (2012); B. Zenker, H. Fehske, H. Beck, C. Monney, and A.R. Bishop, Phys. Rev. **B88**, 075138 (2013); G. Monney, C. Monney, B. Hildebrand, P. Aebi, and H. Beck, Phys. Rev. Lett. **114**, 086402 (2015); H. Watanabe, K. Seki, and S. Yunoki, Phys. Rev. **B91**, 205135 (2016).
- [8] I. Wakisaka, T. Sudayama, K. Takubo, T. Mizokawa. M. Arita, H. Namatame, M. Taniguchi, N. Katayama, M. Nohara, and H. Takagi, Phys. Rev. Lett. **103**, 026402 (2009).
- [9] A. Perali, D. Neilson and A.R. Hamilton, Phys. Rev. Lett. **110**, 146803 (2013).
- [10] L.M. Falicov and J.C. Kimball, Phys. Rev. Lett. **22**, 997 (1969).
- [11] C. D. Batista, Phys. Rev. Lett. **89**, 166403 (2002).

- [12] C. D. Batista, J. E. Gubernatis, J. Bonca a H. Q. Lin, Phys. Rev. Lett. **92**, 187601 (2004).
- [13] B. Zenker, D. Ihle, F. X. Bronold, and H. Fehske, Phys. Rev. B **81**, 115122 (2010).
- [14] V. N. Phan, K. W. Becker, and H. Fehske, Phys. Rev. B **81**, 205117 (2010).
- [15] K. Seki, R. Eder, and Y. Ohta, Phys. Rev. B **84**, 245106 (2011).
- [16] B. Zenker, D. Ihle, F. X. Bronold, and H. Fehske, Phys.Rev. B **85**, 121102R (2012).
- [17] T. Kaneko, K. Seki, and Y. Ohta, Phys. Rev. B **85**, 165135 (2012).
- [18] T. Kaneko, S. Ejima, H. Fehske, and Y. Ohta, Phys. Rev. B **88**, 035312 (2013).
- [19] S. Ejima, T. Kaneko, Y. Ohta and H. Fehske, Phys. Rev. Lett. **112**, 026401 (2014).
- [20] P. Farkašovský, EPL **110**, 47007 (2015).
- [21] P. Farkašovský, Phys. Rev. B **95**, 045101 (2017).
- [22] G. Czycholl, Phys. Rep. B **143**, 277 (1986).
- [23] B. Zenker, H. Fehske, and C.D. Batista, Phys.Rev. B **82**, 165110 (2010).
- [24] P. M. R. Brydon, J. X. Zhu, M. Gulacsi, A. R. Bishop, Phys. Rev. B **72**, 125122 (2005).
- [25] C.E.T. Goncalves da Silva and L.M.Falicov, Solid State Commun. **17**, 1521 (1975); P. Farkašovský, Phys. Rev. B **52**, R5463 (1995); P. Farkašovský, Acta Physica Slovaca **60**, 497 (2010).
- [26] S. R. White, Phys. Rev. Lett. **69**, 2863 (1992).